



## Electron beam adaptation measurement of an infrared FEL

J.-M. Ortega\*, B. Rieul, J.-P. Berthet, F. Glotin, R. Prazeres

LCP, Bat 201 P. 2 Orsay 91405, France

### ARTICLE INFO

#### Article history:

Received 9 October 2012

Received in revised form

3 December 2012

Accepted 25 December 2012

Available online 3 January 2013

#### Keywords:

Free-electron laser

Undulator beam adaptation

Beam size measurement

### ABSTRACT

We have studied the electron beam transverse adaptation in an FEL oscillator in a very large interval of wavelength (3 to 150  $\mu\text{m}$ ) and electron energy range (12 to 45 MeV). Beam dimensions are measured by a moving wire whose temperature dependent resistivity is monitored. By a fast motion of the wire we measure its temperature increase at each transverse position before thermal equilibrium takes place. The beam profile is then directly proportional to the series of the measured values. The results fits well the analytical theory of FEL beam adaptation, even when the undulator vacuum chamber is used as an optical waveguide.

© 2012 Elsevier B.V. All rights reserved.

### 1. Introduction

In a free electron laser, the optimized optical power,  $P_{\text{opt}}$ , depends on the so-called optical SSG (Small Signal Gain) at the start of the amplification process. A simplified small gain formula shows the electron beam parameters that can be varied to optimize the optical gain:

$$G_{\text{laser}} \approx \frac{I_{pp}}{\Sigma_e + \Sigma_o} F_{\text{inh}}(\sigma_\gamma, \sigma_x, \sigma_y, \sigma_{\theta x}, \sigma_{\theta y}) \quad (1)$$

where  $F_{\text{inh}}$  is a function depending on the energy spread,  $\sigma_\gamma$ , the beam transverse dimensions,  $\sigma_x$ ,  $\sigma_y$  and respective divergence,  $\sigma_{\theta x}$  and  $\sigma_{\theta y}$ .  $I_{pp}$  is the peak current and  $\Sigma_e$  and  $\Sigma_o$  are respectively the electron and the optical beam cross-section areas, assuming Gaussian beams. The laser power is optimized [1] by improving as much as possible the peak current, the emittance (acting on  $F_{\text{inh}}$ ) and the beam sizes. For low (optical) gain FELs, as much of the infrared ones, the optimization of the gain at short wavelengths is achieved by minimizing the surface ( $\Sigma_e$ ) of the electron beam along the undulator [2–4] (the surface of the optical beam being determined by the cavity mirrors). The results of this well-known optimization is displayed in Section 3 with the numerical values of interest. For high gain, in particular single pass (SASE), FELs, beam matching is different and has been studied by many authors [5,6].

Here, we are interested in the beam matching in low gain infrared FELs. At relatively short wavelength (typically  $< 30$  to  $40 \mu\text{m}$ ), the above optimization is expected to work. However, since, to our knowledge, there are no published measurements, it is part of our study to demonstrate experimentally this approach in this range. The other part deals with the long wavelength

range. A particularity of these lasers is that, at longer wavelengths, diffraction losses take place since the diffraction limited optical beam becomes larger than the undulator vacuum chamber. To alleviate partially this effect we use the undulator vacuum chamber as an optical waveguide by focusing the beam at its ends [7]. The guiding occurs only in this vacuum chamber and free space propagation occurs between it and the cavity mirrors. The output laser power exhibit then spectral holes that are characteristics of this configuration. They were reproduced satisfactorily by numerical simulations [7]. Therefore, it could happen that a standard adaptation of the electron beam could not fit this configuration and that the optimized size can be different. In order to address this problem, we have measured the electron beam profiles at different energies and compared with the standard analytical values.

The CLIO mid-infrared free electron laser (FEL) is a user facility since 1992. It is based on a 3 GHz RF LINAC with a thermo-ionic gun [8]. It has given rise to many FEL developments [9] and applications [[http://clio.lcp.u-psud.fr/clio\\_eng/topics.html](http://clio.lcp.u-psud.fr/clio_eng/topics.html)]. CLIO is designed to operate in a large spectral range. This has enabled us to lase from  $3 \mu\text{m}$  at 45 MeV to  $150 \mu\text{m}$  at 12 MeV [10]. Fig. 1 displays the typical average power emitted from the FEL operating at 25 Hz macro-pulse rate. Each macro-pulse is  $10 \mu\text{s}$  long and contain about 600 micro-pulses, a few ps long, separated by 16 ns. The average power up to  $20 \mu\text{m}$  at 32 MeV is about 1 W. It decreases strongly at longer wavelengths due to a lower transmitted electron current and diffraction losses both in the optical cavity and transport beam line.

### 2. Wire scanner principle

There are many imaging techniques [11] of transverse beam profiles used worldwide. In our case, the average beam current is

\* Corresponding author. Tel.: +33 1 6915 3294; fax: +33 1 6915 3328.  
E-mail address: [jean-michel.ortega@u-psud.fr](mailto:jean-michel.ortega@u-psud.fr) (J.-M. Ortega).

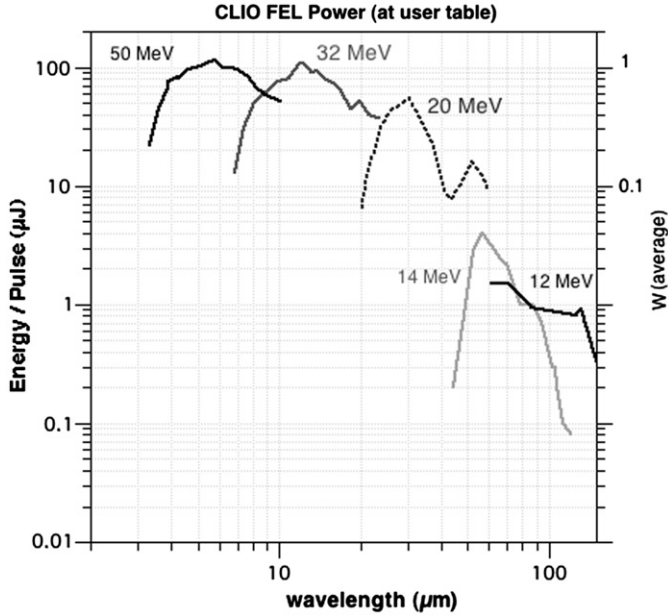


Fig. 1. Spectral range of the infrared FEL CLIO at different energies.

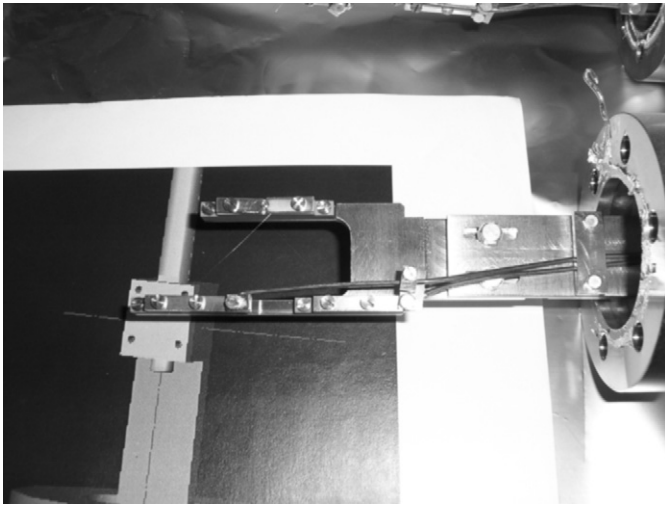


Fig. 2. Photography of the 2 orthogonal tungsten moving wires.

high (20  $\mu\text{A}$ ), leading to almost 1 kW of average power. Therefore we chose a technique intercepting the smallest possible part of the beam. We use wires of diameter of 20  $\mu\text{m}$ . A set of two orthogonal movable wires is installed at entry of the 2 m undulator (Fig. 2). During displacement, the intercepted part of the beam produces a current of secondary electrons [12] and a variation of the wire resistance [13]. The accelerator having notable parasitic beam losses, which produce noise in the secondary electron emission, it appeared impossible to use phenomenon. Therefore, we opted for the second method, i.e., measuring the wire resistance variations.

In a previous paper [12] we discussed measurements made by moving slowly the wire across the beam, so as to have thermal equilibrium, and recording its resistance increase. In this case, in order to correlate the measurements with the size of the beam, we had to make assumptions on the cooling processes of the wire. For simplicity, we assumed that black body radiation was dominant, and it appeared that the results cannot be considered as reliable and, indeed, did not fit the theory. Attempts to perform more sophisticated calculations including thermal cooling along

the wires were not conclusive, since the shape of the electron beam is not known a priori. Therefore, we implemented a new measurement method that we describe in this study: By fast moving the wire we measure its temperature-induced resistance increase for each macro-pulse at a different transverse position. This produces an easily measurable signal, by the fact we have a high current accelerator. Each macro-pulse contains approximately  $3 \times 10^{12}$  particles, i.e., 0.5  $\mu\text{C}$  and produces a resistance variation between typically 0.1 to 0.01  $\Omega$ . These variations appear as a series of peaks superimposed on a global warming of the wire (Figs. 3 and 4). The beam profile is then directly proportional to the series of recorded values, as we show below.

There are 2 quadrupoles used to adapt the beam in the 2 m long CLIO undulator. These quadrupoles are located respectively at 80 and 35 cm from the undulator entrance. After a first adjustment calculated to match roughly the standard matching, they are adjusted at each energy in order to produce the maximum FEL power, without any other consideration. The resulting beam sizes are displayed on Fig. 5.

In order to evaluate the magnitude of resistance variations, we assumed first that the beam has a Gaussian elliptical shape whose axis is oriented along the horizontal and vertical direction. The parameters of the tungsten wires are shown on Table I. A beam of  $N$  particles, centered at coordinate (0,0), crossing the wire at coordinate (x,y) loses an energy:

$$dw_d(x,y) = dx dy \frac{N \alpha \rho}{2\pi\sigma_x\sigma_y} \left(\frac{dE}{dx}\right) \exp\left(-\frac{x^2}{2\sigma_x^2} - \frac{y^2}{2\sigma_y^2}\right) \quad (2)$$

When the wire is located at the center of the beam, the energy deposited increases locally the temperature of the wire by a maximum of:

$$\Delta T(0,y) = \frac{dw_d(0,y)}{\rho C_p dx dy} = \frac{N}{2\pi\sigma_x\sigma_y C_p} \left(\frac{dE}{dx}\right) \exp\left(-\frac{y^2}{2\sigma_y^2}\right) \quad (3)$$

For one CLIO macro-pulse at 44 MeV,  $N \approx 3 \times 10^{12}$ ,  $\sigma_x = 0.7$  mm and  $\sigma_y = 1.2$  mm, it comes:

$$\Delta T(0,0) = 95\text{K} \quad (4)$$

The local resistance of the portion of wire of length  $dy$  is:

$$r = (R_T/L) dy \quad (5)$$

where  $R_T$  (21  $\Omega$ ) is the total resistance of the wire of length  $L$  (6 cm)

The local variation of resistance is then:

$$r(0,y) = r \alpha \Delta T(0,y) = \frac{R_T dy}{L} \frac{\alpha N}{2\pi\sigma_x\sigma_y C_p} \left(\frac{dE}{dx}\right) \exp\left(-\frac{y^2}{2\sigma_y^2}\right) \quad (6)$$

where  $\alpha$  is the  $W$  temperature coefficient

Integrating over the wire length:

$$\Delta R_T(x=0) = \int_y r(0,y) = \frac{\alpha N R_T}{\sqrt{2\pi}\sigma_x L C_p} \left(\frac{dE}{dx}\right)$$

and

$$\Delta R_T(x) = \Delta R_T(x=0) \exp\left(-\frac{x^2}{2\sigma_x^2}\right) \quad (7)$$

One finds

$$\Delta R_T(x=0) \approx 0.45\Omega \quad (8)$$

The experimental value is close to 0.25  $\Omega$ . The difference seems to be due to a beam halo, visible on the curves (Figs. 3 and 4). This produces wings on the distribution so that 40% of the particles are not located in a Gaussian envelope.

The maximum resistance variation, due to the interplay between accumulated macro-pulses and cooling, is approximately 4  $\Omega$ .

Download English Version:

<https://daneshyari.com/en/article/1823312>

Download Persian Version:

<https://daneshyari.com/article/1823312>

[Daneshyari.com](https://daneshyari.com)